Progress In Electromagnetics Research M, Vol. 24, 29–44, 2012

ANALYTICAL COMPUTATION OF RELUCTANCE SYNCHRONOUS MACHINE INDUCTANCES UNDER DIFFERENT ECCENTRICITY FAULTS

H. Akbari*

Department of Electrical Engineering, Yazd Branch, Islamic Azad University, Yazd, Iran

Abstract—In the previous works, based on winding function theory, the calculation of reluctance machine inductances is carried out using numerical integration or inexact analytical equations based on approximated Fourier series expansions of the inverse air gap function. In this paper, development in Fourier series of the inverse air gap function has not been used, but a closed form analytical equation is developed for inductances calculation. This leads to a very precise computation of the inductances of the faulted machine and more accurate results. Moreover, all space harmonics ignored by the Fourier series expansions of the inverse air gap function will be included in the model. Derived comprehensive equation allows calculating time varying inductances of reluctance machines with different static, dynamic and mixed eccentricities in the frame of a single program. Inductances obtained by the proposed method are compared to those obtained from FE results. A satisfactory match was found between them.

1. INTRODUCTION

The mechanical faults are responsible for more than 50% of all failures in electrical machines. The most important mechanical fault is eccentricity [1]. Machine eccentricity is the condition of unequal air gap that exists between the stator and rotor. Many electrical and mechanical faults in the no-load operation of the motor lead to the eccentricity between the rotor and stator [2]. Relatively small amount of eccentricity can have a significant impact on the operational life of bearings.

Received 20 October 2011, Accepted 29 February 2012, Scheduled 13 March 2012

* Corresponding author: Hamidreza Akbari (hamid_r_akbari@yahoo.com).

So far, magnetic equivalent circuit, finite element and winding function approaches have been used for modeling and analysis of electrical machines with different kinds of faults. Magnetic equivalent circuit method needs shorter computation time compared with the finite element method, but it is less accurate. In this method, the magnetic equivalent circuit is introduced for all sections of the machine [3, 4]. Studying faulty electrical machines needs precise mathematical models and this method is not capable to diagnose the fault in the real cases [1, 2]. The finite element method is based on the magnetic field distribution and is suitable tool for analysis of faulty machines considering complicated and non-linear behavior of the machine [5]. Although, this approach gives accurate results, however this method is time consuming especially for the analysis of electrical machines with asymmetry in the motor body such as eccentricity. Moreover it requires an extensive characterization of the machine, for example, electromagnetic properties of all the materials making up the machine and the physical geometry [1, 5–9].

Winding function approach is based on the basic geometry and winding layout of machine [10]. The only information required in winding function approach is the winding layout and machine geometry. One advantage of this method is that the study of the behavior of any machine with any winding distribution and air gap length is possible. Hence this method has found application in the analysis of fault conditions in machines, such as broken rotor bars [11] and fault condition in stator windings [12]. The modified winding function approach (MWFA) for asymmetrical air gap in a salient pole synchronous machine has been proposed in [13]. This theory has been applied to analyze static, dynamic and mixed eccentricity in induction and synchronous machines [14–18]. An essential step of this method is the calculation of machine inductances. Many have calculated these inductances by taking into account the influence of spatial harmonics due to winding distribution and slotting effect. An accurate inductances calculation is necessary to improve the accuracy of the analysis of electrical machines.

In the previous works, based on winding function theory, the calculation of reluctance machine inductances is carried out using numerical integration or inexact analytical equations based on approximated Fourier series expansions of the inverse air gap function [19–23]. In this study, development in Fourier series of the inverse air gap function has not been used, but a closed form analytical equation is obtained. It is clear that the proposed technique decreases the time and computation process and leads to more accurate results. Derived analytical equation prevents the imprecision caused

by numerical differentiations. The proposed method allows calculating time varying inductances of reluctance machines with different static, dynamic and mixed eccentricities in the frame of a single program.

The author in the previous works modeled induction machines and synchronous machines under different eccentricity conditions utilizing winding function approach [17, 18, 24]. In this paper, analytical expressions for inductances and their derivatives are established.

The contributions of the present paper includes: 1) Introducing a precise geometrical model of reluctance machines under general eccentricity fault; including static, dynamic and mixed eccentricities, 2) Defining the inverse air gap function of the eccentric reluctance machine and determining its indefinite integral, 3) Developing a new closed form analytical expression for calculation of reluctance machine inductances under different types of eccentricities and 4) Determining an analytical expression for derivative of inductances.

2. WINDING FUNCTION ANALYSIS

An elementary reluctance machine scheme is presented in Fig. 1.

There are no restrictions about windings distribution for the analysis. Furthermore, restrictions over the air gap eccentricity are not assumed. Starting from an arbitrary closed path *abca,* a modification of the winding function approach which considers the air gap non-uniformity derives [13].

Points a and c are located on the stator while b is located on the rotor. By applying the Ampere's law over the closed path, shown in Fig. 1 and using Gauss's law for magnetic field, the modified winding

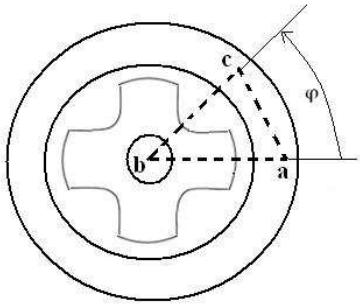

Figure 1. Cross section of a reluctance synchronous machine.

function (MWF) can be expressed as in (1) [13]

$$M(\varphi,\theta) = n(\varphi,\theta) - \frac{\int_0^{2\pi} g^{-1}(\varphi,\theta)\, n(\varphi,\theta) d\varphi}{\int_0^{2\pi} g^{-1}(\varphi,\theta) d\varphi} \tag{1}$$

where, φ is arbitrary angle in stator reference frame, θ is rotor position angle and g^{-1} is inverse air gap function. The function $n(\varphi,\theta)$ is called the turns function. This function represents the number of the winding turns enclosed by the closed path. The permeability of the stator and rotor iron cores is assumed to be infinite when compared to the permeability of the air gap. When the air gap distribution is uniform, (1) can be simplified as follows:

$$M(\varphi,\theta) = n(\varphi,\theta) - < n(\varphi,\theta) > \tag{2}$$

Operator $< f >$ is defined as the mean of function f over $[0 - 2\pi]$. However, (2) is not valid for a non-uniform air gap. For analysis of reluctance machines which have non-uniform air gap, (1) should be used. Magnetomotive force distribution in the air gap, produced by current i_A of winding A, can simply be found by product of $M(\varphi,\theta)$ from (1) and the current flowing in the winding.

$$F_A(\varphi,\theta) = M_A(\varphi,\theta) i_A \tag{3}$$

The differential flux through a differential area in the air gap, $lrd\varphi$, can be written as follows:

$$d\varphi = F_A(\varphi,\theta) \frac{\mu_0 lr d\varphi}{g(\varphi,\theta)} \tag{4}$$

where, r is mean radius and l is axial stack length of the machine. Integrating the differential flux in the region covered by either a stator coil or rotor coil, yields:

$$\varphi_{BA} = \mu_0 lr \int_{\varphi_1}^{\varphi_2} F_A(\varphi,\theta)\, g^{-1}(\varphi,\theta)\, d\varphi \tag{5}$$

$n_B(\varphi,\theta)$ is equal to the coil turns in the region $(\varphi_1 < \varphi < \varphi_2)$ and zero otherwise. Therefore the total flux linking coil B due to current in winding A, λ_{BA}, is obtained from multiplying (5) by $n_B(\varphi,\theta)$ and integrating it over the whole surface.

$$\lambda_{BA} = \mu_0 lr \int_0^{2\pi} n_B(\varphi,\theta)\, F_A(\varphi,\theta)\, g^{-1}(\varphi,\theta)\, d\varphi \tag{6}$$

The mutual inductance of windings A and B, due to current i_a in the coil A (L_{BA}), is

$$L_{BA} = \frac{\lambda_{BA}}{i_A} \tag{7}$$

Therefore, the general expression for mutual inductance between any two windings A and B in any electrical machine is

$$L_{BA} = \mu_0 lr \int_0^{2\pi} n_B(\varphi,\theta) M_A(\varphi,\theta) g^{-1}(\varphi,\theta) d\varphi \tag{8}$$

Inductances of salient pole machine can be calculated from (8) using geometrical characteristic of the machine. Mechanical asymmetry and faults of stator and rotor windings can be simulated by this technique.

3. MODELING OF DIFFERENT KINDS OF ECCENTRICITIES IN RELUCTANCE MACHINES

In an ideal machine, three geometric axes; stator (A_s), rotor (A_r) and rotation (A_c) coincide with each other. The occurrence of eccentricity means the displacement of stator geometric axis and rotor geometric axis. Obviously, the winding functions of the machine windings don't change in eccentricity conditions compared to the symmetrical conditions. However, the function of the air gap length will change with respect to the symmetrical case.

There are three types of air gap eccentricity; Static, dynamic and mixed eccentricity [4]. Static eccentricity (SE) occurs when the rotor rotates about its own centerline, but this centerline does not coincide with that of the stator bore. Static eccentricity in an elementary reluctance machine is presented in Fig. 2.

The air gap length variation under SE for salient pole synchronous machines can be described by air gap functions in polar and interpolar

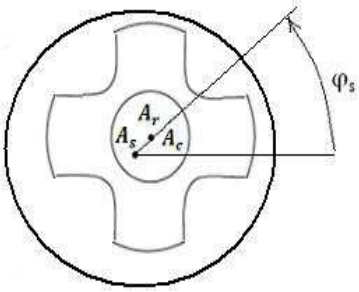

Figure 2. Static eccentricity in a reluctance machine.

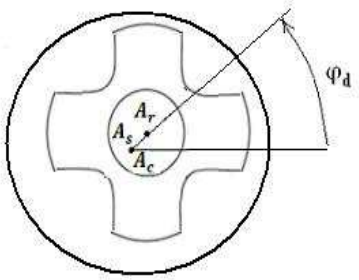

Figure 3. Dynamic eccentricity in a reluctance machine.

regions as follows:

$$g_d(\varphi, \varphi_s, \delta_s) = g_0(1 - \delta_s \cos(\varphi - \varphi_s)) \quad (9)$$

$$g_q(\varphi, \varphi_s, \delta_s) = g_1(1 - \delta_s \cos(\varphi - \varphi_s)) \quad (10)$$

where the subscripts d and q refer to the polar and inter-polar regions, respectively. δ_s is static eccentricity coefficient, φ_s is angle at which rotation and stator axes are separated and g_0 and g_1 are effective air gap length in polar and interpolar regions, respectively. The stator slots effect is included by Carter's coefficient referred to the slots [25].

Dynamic eccentricity (DE) occurs when the rotor geometric center is not at the center of rotation, producing consequently an air gap periodic variation as a rotor position function. Fig. 3 shows dynamic eccentricity in a reluctance machine.

The air gap length variation under DE for reluctance machines can be described by air gap functions in polar and interpolar regions as follows:

$$g_d(\varphi, \varphi_s, \delta_s) = g_0(1 - \delta_d \cos(\varphi - \varphi_d)) \quad (11)$$

$$g_q(\varphi, \varphi_s, \delta_s) = g_1(1 - \delta_d \cos(\varphi - \varphi_d)) \quad (12)$$

where δ_d is dynamic eccentricity coefficient and φ_d is angle at which rotation and rotor axes are separated.

In mixed eccentricity (ME) both rotor and rotation axes are displaced individually in respect to the stator axis. Mixed eccentricity in a reluctance synchronous machine is presented in Fig. 4.

In ME condition, air gap function can be represented by

$$g_d = g_0(1 - \delta_s \cos(\varphi - \varphi_s) - \delta_d \cos(\varphi - \varphi_d)) \quad (13)$$

$$g_q = g_1(1 - \delta_s \cos(\varphi - \varphi_s) - \delta_d \cos(\varphi - \varphi_d)) \quad (14)$$

Through geometric analysis on Fig. 4, it is straight forward to show that

$$\sin(\varphi_m - \varphi_s) = \frac{\delta_d \sin(\varphi_d - \varphi_s)}{\delta} \quad (15)$$

Therefore

$$\varphi_m = \varphi_s + \sin^{-1}\left(\frac{\delta_d \sin(\varphi_d - \varphi_s)}{\delta}\right) \quad (16)$$

and

$$\delta = \left[{\delta_s}^2 + {\delta_d}^2 + 2\delta_s \delta_d \cos(\varphi_d - \varphi_s)\right]^{\frac{1}{2}} \quad (17)$$

where δ is general eccentricity factor and φ_m is angle at which rotor and stator centers are separated. In the case of SE, $\delta_d = 0$ and in DE, $\delta_s = 0$.

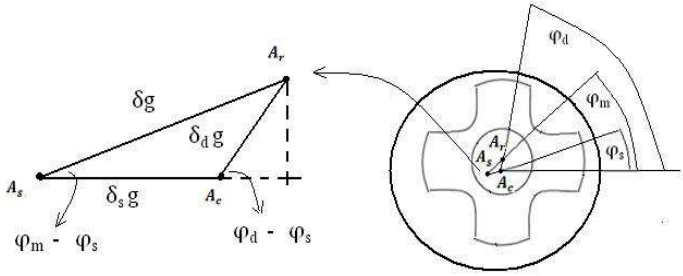

Figure 4. Mixed eccentricity in a reluctance machine.

4. ANALYTICAL EXPRESSIONS FOR INDUCTANCES AND THEIR DERIVATIVES

Calculation of inductances by (8) requires that explicit expressions for the inverse air gap function be obtained. Generally, in calculating salient pole machine inductances, approximated Fourier series expansions of the inverse air gap function are used. To enhance the accuracy of calculated inductances, more terms of Fourier series expansion must be included. This makes the calculation more complex.

In this investigation, analytical expressions for inductances of eccentric reluctance synchronous machines and their derivatives are derived without any development in Fourier series. It is clear that the proposed technique decreases the time and computation process and leads to more accurate results.

To obtain the analytic equations, it is assumed that the functions f_d and f_q are indefinite integrals of the functions $g_d^{-1}()$ and $g_q^{-1}()$, respectively as follows:

$$f_d(\varphi, \varphi_m, \delta) = \int g_d^{-1}(\varphi, \varphi_m, \delta)\, d\varphi = \int \frac{1}{g_0(1 - \delta\cos(\varphi - \varphi_m))} d\varphi \quad (18)$$

$$f_q(\varphi, \varphi_m, \delta) = \int g_q^{-1}(\varphi, \varphi_m, \delta)\, d\varphi = \int \frac{1}{g_1(1 - \delta\cos(\varphi - \varphi_m))} d\varphi \quad (19)$$

These expressions are elaborated to yield

$$f_d(\varphi, \varphi_m, \delta) = \frac{1}{g_0\sqrt{1-\delta^2}} \cos^{-1}\left(\frac{\cos(\varphi - \varphi_m) - \delta}{1 - \delta\cos(\varphi - \varphi_m)}\right) \quad (20)$$

$$f_q(\varphi, \varphi_m, \delta) = \frac{1}{g_1\sqrt{1-\delta^2}} \cos^{-1}\left(\frac{\cos(\varphi - \varphi_m) - \delta}{1 - \delta\cos(\varphi - \varphi_m)}\right) \quad (21)$$

It is assumed that the functions f_1 and f_2 to be the definite

integrals as follows:

$$f_1(\varphi_m, \theta, \delta) = \int_0^{2\pi} g^{-1}(\varphi, \varphi_m, \theta, \delta) d\varphi \tag{22}$$

$$f_2(\varphi_m, \theta, \delta) = \int_0^{2\pi} g^{-1}(\varphi, \varphi_m, \theta, \delta) n_b(\varphi) d\varphi \tag{23}$$

The air gap functions in polar and interpolar regions are described by g_d and g_q, respectively. Separating the associated terms of polar and interpolar regions and referring to Fig. 5, (22) results in

$$f_1(\varphi_m, \theta, \delta) = \sum_{i=1}^{p} \left(\int_{\theta+(i-1)\theta_d+(i-1)\theta_q}^{\theta+i\theta_d+(i-1)\theta_q} g_d^{-1}(\varphi, \varphi_m, \delta) d\varphi + \int_{\theta+i\theta_d+(i-1)\theta_q}^{\theta+i\theta_d+i\theta_q} g_q^{-1}(\varphi, \varphi_m, \delta) d\varphi \right) \tag{24}$$

where θ is rotor position angle in stator reference frame.

Using the definitions given in (18) and (19), f_1 can be obtained.

$$\begin{aligned} & f_1(\varphi_m, \theta, \delta) \\ = & \sum_{i=1}^{p} (f_d(\theta + i\theta_d + (i-1)\theta_q, \varphi_m, \delta) - f_d(\theta + (i-1)\theta_d + (i-1)\theta_q, \varphi_m, \delta) \\ & + f_q(\theta + i\theta_d + i\theta_q, \varphi_m, \delta) - f_q(\theta + i\theta_d + (i-1)\theta_q, \varphi_m, \delta)) \end{aligned} \tag{25}$$

where f_d and f_q are calculated from (20) and (21). In a similar way, f_2 is calculated in the whole range of φ. Function f is defined as follows:

$$f(\varphi_m, \theta, \delta) = \frac{f_2(\varphi_m, \theta, \delta)}{f_1(\varphi_m, \theta, \delta)} \tag{26}$$

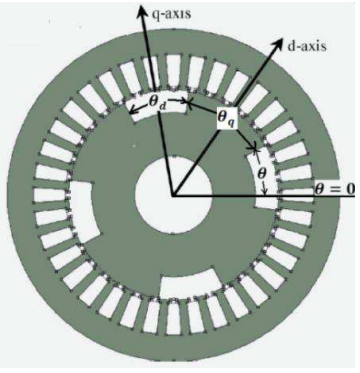

Figure 5. Cross section of an elementary reluctance machine [19].

Considering (1), (22), (23) and (26), MWF of stator phase b, M_b, is derived as

$$M_b(\varphi, \varphi_m, \theta, \delta) = n_b(\varphi) - f(\varphi_m, \theta, \delta) \tag{27}$$

Replacing (27) in (8) and separating the associated terms of polar and interpolar regions, L_{ab} is obtained as follows:

$$L_{ab} = \mu_\circ lr \sum_{i=1}^{p} \left[\int_{\theta+(i-1)\theta_d+(i-1)\theta_q}^{\theta+i\theta_d+(i-1)\theta_q} g_d^{-1}(\varphi, \varphi_m, \theta, \delta) n_a(\varphi)(n_b(\varphi) - f(\varphi_m, \theta, \delta)) d\varphi \right.$$
$$\left. + \int_{\theta+i\theta_d+(i-1)\theta_q}^{\theta+i\theta_d+i\theta_q} g_q^{-1}(\varphi, \varphi_m, \theta, \delta) n_a(\varphi)(n_b(\varphi) - f(\varphi_m, \theta, \delta)) d\varphi \right] \tag{28}$$

where a and b are accounted for the stator phases. It is assumed that, $\varphi_{x_{2k-1}}$ to $\varphi_{x_{2k}}$ are the stator slots being in polar region ($\varphi_{x_{2k}} - \varphi_{x_{2k-1}} = \theta_d$) and $\varphi_{x_{2k}}$ to $\varphi_{x_{2k+1}}$ are the stator slots being in interpolar region ($\varphi_{x_{2k+1}} - \varphi_{x_{2k}} = \theta_q$). Therefore

$$L_{ab} = \mu_\circ lr \sum_{k=1}^{p} \left[\sum_{i=x_{2k-1}}^{i=x_{2k}} n_a(\varphi_{ti})(n_b(\varphi_{ti}) - f(\varphi_m, \theta, \delta)) \int_{\varphi_i}^{\varphi_{i+1}} g_d^{-1}(\varphi, \varphi_m, \delta) d\varphi \right.$$
$$\left. + \sum_{i=x_{2k}}^{i=x_{2k+1}} n_a(\varphi_{ti})(n_b(\varphi_{ti}) - f(\varphi_m, \theta, \delta)) \int_{\varphi_i}^{\varphi_{i+1}} g_q^{-1}(\varphi, \varphi_m, \delta) d\varphi \right] \tag{29}$$

where φ_i is angle of stator slot i center, φ_{ti} is angular position between stator slot i and stator slot $i+1$ (angle of stator tooth i). $\varphi_{x_{2k-1}}$, $\varphi_{x_{2k}}$ and $\varphi_{x_{2k+1}}$can be easily determined at every time step of simulation. Considering (18) and (19), L_{ab} is obtained as follows:

$$L_{ab} = \mu \circ lr \sum_{k=1}^{p} \left[\sum_{i=x_{2k-1}}^{i=x_{2k}} \right.$$
$$[n_a(\varphi_{ti})(n_b(\varphi_{ti}) - f(\varphi_m, \theta, \delta))(f_d(\varphi_{i+1}, \varphi_m, \delta) - f_d(\varphi_i, \varphi_m, \delta))] +$$
$$\left. \sum_{i=x_{2k}}^{i=x_{2k+1}} n_a(\varphi_{ti})(n_b(\varphi_{ti}) - f(\varphi_m, \theta, \delta))(f_q(\varphi_{i+1}, \varphi_m, \delta) - f_q(\varphi_i, \varphi_m, \delta)) \right] \tag{30}$$

where f_d and f_q are calculated from (20) and (21), respectively.

Functions f, f_q and f_d depend on θ because φ_m and δ are θ-dependent. Therefore, the derivative of L_{ab} versus θ is determined as

Table 1. Specifications of the simulated machine.

Pole arc (degrees)	57
Inner radius of stator (mm)	80
Air gap length (mm)	0.6
Active axial length (mm)	130
Number of turns per slot	20
Number of stator slots	30
Stator slot pitch (degrees)	12
Rotor outer radius (mm)	79.4

follows:

$$\frac{\partial L_{ab}}{\partial \theta} = \mu \circ lr \sum_{k=1}^{p} \left[\sum_{i=x_{2k-1}}^{i=x_{2k}} \left[n_a(\varphi_{ti}) \left(n_b(\varphi_{ti}) - f(\varphi_m, \theta, \delta) \right) \left(\frac{\partial f_d(\varphi_{i+1}, \varphi_m, \delta)}{\partial \theta} - \frac{\partial f_d(\varphi_i, \varphi_m, \delta)}{\partial \theta} \right) - n_a(\varphi_{ti}) \frac{\partial f(\varphi_m, \theta, \delta)}{\partial \theta} \right. \right.$$
$$\left. \left(f_d(\varphi_{i+1}, \varphi_m, \delta) - f_d(\varphi_i, \varphi_m, \delta) \right) \right] + \sum_{i=x_{2k}}^{i=x_{2k+1}} \left[n_a(\varphi_{ti}) \right.$$
$$\left(n_b(\varphi_{ti}) - f(\varphi_m, \theta, \delta) \right) \left(\frac{\partial f_q(\varphi_{i+1}, \varphi_m, \delta)}{\partial \theta} - \frac{\partial f_q(\varphi_i, \varphi_m, \delta)}{\partial \theta} \right)$$
$$\left. \left. - n_a(\varphi_{ti}) \frac{\partial f(\varphi_m, \theta, \delta)}{\partial \theta} \left(f_q(\varphi_{i+1}, \varphi_m, \delta) - f_q(\varphi_i, \varphi_m, \delta) \right) \right] \right] \quad (31)$$

Derived analytical equation prevents the imprecision caused by numerical differentiations.

5. COMPUTATION OF INDUCTANCES

In this section, the inductances of a reluctance synchronous machine whose parameters are given in Table 1, are computed under healthy and different eccentricity conditions. Inductances are calculated by means of obtained analytical equation and determined geometrical models. It should be noted that magnetic saturation and leakage flux have not been considered.

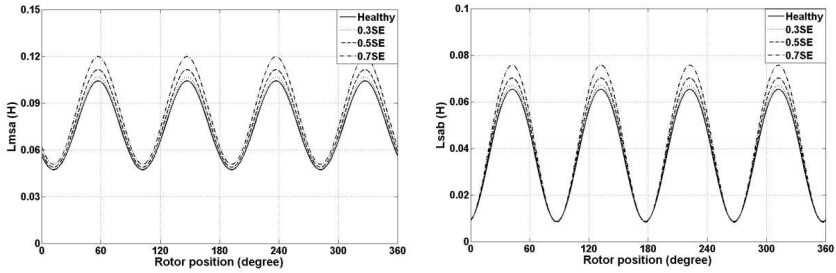

Figure 6. (a) Calculated magnetizing inductance of stator phase A and (b) mutual inductance between stator phase A and stator phase B under different SE conditions.

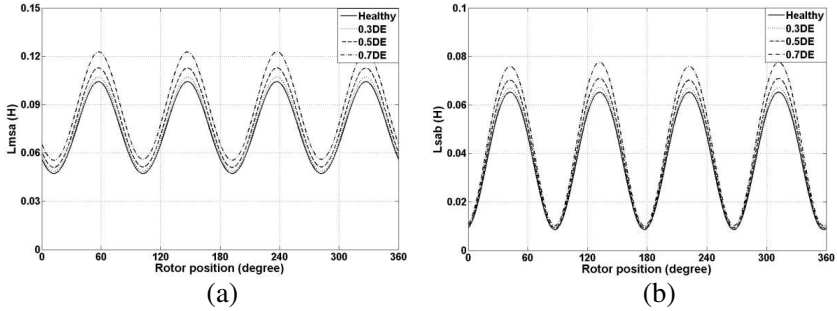

Figure 7. (a) Calculated magnetizing inductance of stator phase A and (b) mutual inductance between stator phase A and stator phase B under different DE conditions.

The profiles of magnetizing inductance of stator phase A and mutual inductance between phase A and B of stator under different eccentricity conditions are shown in Figs. 6, 7 and 8. Comparison of plots in these figures show how SE, DE and ME affect the profile of magnetizing and mutual inductances. ME causes asymmetrical magnetizing and mutual inductances, whereas, DE and SE cause symmetrical inductances. In the cases of DE and SE, by increasing the eccentricity severity, the magnitude of these inductances increases. The rate of increase of the magnetizing inductance is higher than that of the mutual inductance. Referring to Fig. 8 it is seen that the asymmetry occurred in the magnetizing inductance in the case of ME is higher than that of the mutual inductance.

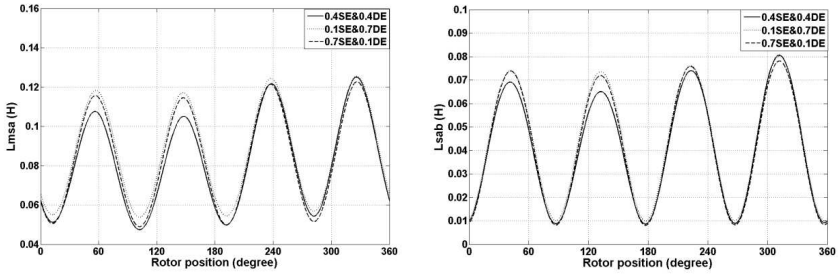

Figure 8. (a) Calculated magnetizing inductance of stator phase A and (b) mutual inductance between stator phase A and stator phase B under different ME conditions.

Table 2. Specifications of a reluctance synchronous machine [19].

Pole arc/pole pitch	0.57
Inner radius of stator (mm)	40.3
Air gap length (mm)	0.3
Active axial length (mm)	75
Number of turns per slot	58
Number of stator slots	36
Stator slot pitch (degrees)	10
Rotor outer radius(mm)	40

6. COMPARISON WITH FINITE ELEMENT RESULTS

In order to validate the proposed method, the inductances of a reluctance synchronous machine whose parameters are given in the Table 2, is compared with FE results. A 2-D finite element analysis was used to determine the inductances of stator windings [19]. The magnetic saturation was neglected in order to match the winding function model which considers infinite permeability.

The plots of magnetizing inductance of stator phase A and mutual inductance between stator phase A and stator phase B obtained from FE method and proposed method are shown in Figs. 9 and 10.

The results from the FE method, shown in Fig. 9, can be compared with those in Fig. 10, obtained by the proposed method. The small ripple which is present in the inductances profiles in Fig. 10 is due to MMF variations across the slots. Minimum and maximum values

Table 3. Minimum and maximum values of inductances from two methods (proposed method — FE method).

	max-value (Henry)	**min-value (Henry)**
Lsaa	0.263–0.275	0.175–0.180
Lsab	0.043–0.039	−0.21–−0.215

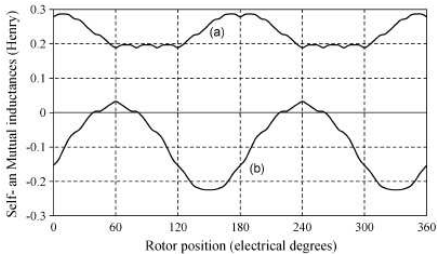

Figure 9. Self inductance of stator phase A (a) and mutual inductance between stator phase A and stator phase B (b) using FE method [19].

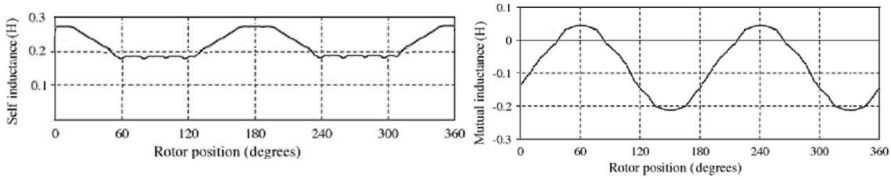

Figure 10. (a) Calculated self inductance of stator phase A and (b) mutual inductance between stator phase A and stator phase B using proposed technique.

of inductances from two methods are summarized in Table 3. The comparison indicates a good agreement between these two results. The main reason for good agreement between the proposed method results and the FE results is that in the proposed method, development in Fourier series of the inverse air gap function has not been used, but closed form equations are employed for inductances calculation. With this approach, all space harmonics ignored by the Fourier series expansions of the inverse air gap function will be included in the model. The author plans to apply the calculated inductances in a coupled electromagnetic model of reluctance synchronous machine in the future for fault analysis.

7. CONCLUSION

In this paper, for calculation of reluctance synchronous machine inductances under different eccentricity conditions, a novel closed form analytical expression is developed. For this purpose, the inverse air gap function of the eccentric reluctance machine has been defined and its indefinite integral has then been determined. Derived comprehensive equation allow calculating time varying inductances of reluctance machines with different static, dynamic and mixed eccentricities in the frame of a single program. The comparison between the proposed method and FEM results indicates a good agreement between these two results. The main reason for good agreement is that in the proposed method, development in Fourier series of the inverse air gap function has not been used, but a closed form equation is employed for inductances calculation. This leads to a very precise computation of the inductances of the faulted machine and more accurate results. Moreover, all space harmonics ignored by the Fourier series expansions of the inverse air gap function will be included in the model. The calculated inductances can be applied in a coupled electromagnetic model of reluctance synchronous machine for fault analysis.

ACKNOWLEDGMENT

This work was supported by Islamic Azad University, Yazd Branch, Yazd, Iran.

REFERENCES

1. Faiz, J. and B. M. Ebrahimi, "Mixed fault diagnosis in three-phase squirrel-cage induction motor using analysis of air-gap magnetic field," *Progress In Electromagnetics Research*, Vol. 64, 239–255, 2006.
2. Faiz, J. and B. M. Ebrahimi, "Static eccentricity fault diagnosis in an accelerating no-load three-phase saturated squirrel-cage induction motor," *Progress In Electromagnetics Research B*, Vol. 10, 35–54, 2008.
3. Meshgin-Kelk, H., J. Milimonfared, and H. Toliyat, "Interbar currents and axial fluxes in healthy and faulty induction motors," *IEEE Transactions on Industry Applications*, Vol. 40, No. 1, 128–134, 2004
4. Faiz, J., B. M. Ebrahimi, and M. B. B. Sharifian, "Different faults and their diagnosis techniques in three-phase squirrel-cage

induction motors — A review," *Electromagnetics*, Vol. 26, No. 7, 543–569, 2006.

5. Faiz, J., B. M. Ebrahimi, and M. B. B. Sharifian, "Time stepping finite element analysis of rotor broken bars fault in a three-phase squirrel-cage induction motor," *Progress In Electromagnetics Research*, Vol. 68, 53–70, 2007.
6. Torkaman, H. and E. Afjei, "FEM analysis of angular misalignment fault in SRM magnetostatic characteristics," *Progress In Electromagnetics Research*, Vol. 104, 31–48, 2010.
7. Vaseghi, B., N. Takorabet, and F. Meibody-Tabar, "Transient finite element analysis of induction machines with stator winding turn fault," *Progress In Electromagnetics Research*, Vol. 95, 118, 2009
8. Torkaman, H. and E. Afjei, "Hybrid method of obtaining degrees of freedom for radial air gap length in SRM under normal and faulty conditions based on magnetostatic model," *Progress In Electromagnetics Research*, Vol. 100, 3754, 2010.
9. De Bortoli, M. J., S. J. Salon, and C. J. Slavic, "Effect of rotor eccentricity and parallel winding on induction behavior: A study using finite element analysis," *IEEE Transactions on Magnetics*, Vol. 29, No. 2, 1676–1682, 1993.
10. Toliyat, H., T. A. Lipo, and J. C. White, "Analysis of a concentrated winding induction machine for adjustable speed drive applications, part-1 (motor analysis)," *IEEE Transactions on Energy Conversion*, Vol. 6, 679–692, 1991.
11. Milimonfared, J., H. M. Kelk, A. Der Minassians, S. Nandi, and H. A. Toliyat, "A novel approach for broken bar detection in cage induction motors," *IEEE Transactions on Industry Applications*, Vol. 35, 1000–1006, 1999.
12. Joksimovic, M. G. and J. Penman, "The detection of inter turn short circuits in the stator windings of operating motors," *IEEE Transactions on Industry Application*, Vol. 47, 1078–1084, 2000.
13. Al-Nuaim, N. A. and H. Toliyat, "A novel method for modeling dynamic air-gap eccentricity in synchronous machines based on modified winding function theory," *IEEE Transactions on Energy Conversion*, Vol. 13, 156–162, 1998.
14. Tabatabaei, I., J. Faiz, H. Lesani, and M. T. Nabavi-Razavi, "Modeling and simulation of a salient pole synchronous generator with dynamic eccentricity using modified winding function approach," *IEEE Transactions on Magnetics*, Vol. 40, No. 3, May 2004.

15. Joksimovic, G. M., "Dynamic simulation of cage induction machine with air gap eccentricity," *IEE Proc. Electr. Power Appl.*, Vol. 152, No. 4, 803–811, Jul. 2005.
16. Faiz, J., B. M. Ebrahimi, and M. Valavi, "Mixed eccentricity fault diagnosis in salient pole synchronous generator using modified winding function method," *Progress In Electromagnetics Research B*, Vol. 11, 155–172, 2009.
17. Akbari, H., J. Milimonfared, and H. Meshgin Kelk, "Axial static eccentricity detection in induction machines by wavelet technique," *International Review of Electrical Engineering,* Vol. 5, No. 3, 2010.
18. Akbari, H., H. Meshgin Kelk, and J. Milimonfared, "Extension of winding function theory for radial and axial non-uniform air gap in salient pole synchronous machines," *Progress In Electromagnetics Research*, Vol. 114, 407428, 2011.
19. Lubin, T. and T. Hamiti, "Comparison between finite-element analysis and winding function theory for inductances and torque calculation of a synchronous reluctance machine," *IEEE Transactions on Magnetics*, Vol. 43, No. 8, 2007.
20. Neti, P. and S. Nandi, "Performance analysis of a reluctance synchronous motor under abnormal operating conditions," *Can. J. Elec. Comput. Eng.*, Vol. 33, No. 2, 2008.
21. Hamiti, T., T. Lubin, and A. Rezzoug, "A simple and efficient tool for design analysis of synchronous reluctance motor," *IEEE Transactions on Magnetics*, Vol. 44, No. 12, Dec. 2008.
22. Obe, E. S., "Direct computation of AC machine inductances based on winding function theory," *Energy Conversion and Management*, Vol. 50, 539–542, 2009.
23. Hamiti, T., T. Lubin, L. Baghli, and A. Rezzoug, "Modeling of a synchronous reluctance machine accounting for space harmonics in view of torque ripple minimization," *Mathematics and Computers in Simulation*, Vol. 81, 354–366, 2010.
24. Akbari, H., J. Milimonfared, and H. Meshgin Kelk, "Improved MWFA for computation of salient pole machine inductances," *International Review of Electrical Engineering*, Vol. 5, No. 6, 2593–2600, 2010.
25. Ostovic, V., *Computer Aided Analysis of Electrical Machines, A Mathematical Approach*, Prentice Hall, 1994.